

Experimental study for the properties of Fe_3O_4 dusty plasma using the air in vacuum chamber system

Ala' Fadhil Ahmed

Department of Astronomy and Space, College of Science, University of Baghdad

E-mail: ala.fadil@yahoo.com

Abstract

In this work, we carried out an experimental study of the dusty plasma by taking the dust material Fe_3O_4 with radius of the any grain $0.1\mu m - 0.5\mu m$. In experiment we use air in the vacuum chamber system under different low pressure (0.1-1) Torr. The results illustrated that the present of dust particles in the air plasma did not effect on Paschen minimum which is 0.5 without dust and with Fe_3O_4 dusty grains.

The effect of Fe_3O_4 dust particles on plasma parameters can be notice in direct current system in glow discharge region. The plasma parameters which were studied in this work represent plasma potential, floating potential, electron saturation current, temperature of the electron, the density of the (electron, ion), and Debye length. The measurements of parameters are taken by four cylindrical probes which diagnosed at distance 4cm from the diameter of the cathode in Paschen minimum at pressure 0.5 Torr. The diameter profiles of plasma parameters in the present of dust are non- uniform. Plasma potential and the floating potential of probe becomes more negatively when the dust immersed into plasma region. The electron density increases in the present of dust particle which lead to decrease the electron temperature and Debye length. The behavior of those parameters shows the discharge current and discharge voltage increases without dust while the discharge current and voltage decreases when Fe_3O_4 dust particles embedded.

Keywords

Dusty plasma, Plasma parameters, Fe_3O_4 dust, Plasma sheath, Langmuir probe.

Article info.

Received: Jan. 2015

Accepted: Mar. 2015

Published: Apr. 2015

دراسة تجريبية لخصائص البلازما المغبرة Fe_3O_4 باستخدام الهواء في منظومة الفراغ

آلاء فاضل احمد الراشدي

قسم الفلك والفضاء، كلية العلوم، جامعة بغداد

الخلاصة

في هذا العمل قمنا بدراسة تجريبية للبلازما المغبرة باستخدام دقائق الغبار لمادة Fe_3O_4 التي نصف قطر الحبيبة من $0.1\mu m$ الى $0.5\mu m$. في التجربة استخدمنا الهواء في منظومة الفراغ تحت ضغوط منخفضة (1 - 0.1) torr. حيث أظهرت النتائج أن وجود جسيمات الغبار في البلازما المتولدة في الهواء لم يؤثر في الحد الأدنى لباشن الذي هو 0.5 torr دون الغبار ومع وجود حبيبات الغبار Fe_3O_4 . حيث لاحظنا تأثير دقائق الغبار على معلمات البلازما في منطقة التوهج. معلمات البلازما التي درست في هذا العمل هي جهد البلازما وجهد العائم ودرجة حرارة الإلكترون وكثافة (الإلكترون، أيون) وطول ديبياي حيث يتم أخذ القياسات لمعلمات البلازما من قبل أربعة مسابر اسطوانية الشكل لتشخيص عند المسافة 4cm وضغط 0.5 torr. وان التوزيع القطري لمعلمات البلازما يكون غير منتظم بوجود غبار Fe_3O_4 . وان جهد البلازما والجهد العائم يصبح أكثر سالبية عند دخول الغبار الى منطقة البلازما وان الكثافة الإلكترونية تزداد بوجود الغبار مما تؤدي إلى تقليل في درجة حرارة الإلكترون وطول ديبياي. ويظهر سلوك تلك المعلمة زيادة في تيار وفولتية التفريغ في حالة عدم وجود الغبار في حين تقل من قيم فولتية التفريغ وتيار التفريغ عند وجود غبار Fe_3O_4 .

Introduction

Typical plasmas consisting of electrons and ions or similar particles with large-mass difference essentially cause temporal as well as spatial variations of collective plasma phenomena [1]. However, the space-time parity can be maintained in pair-ion plasmas with equal mass or slightly different masses [2]. Plasmas not only found in naturally occurring plasmas, but are also used for technological applications. In many industries, e.g., integrated-circuit fabrication, since the deposited is strongly damaged by a high-energy electron, a plasma source having no energetic electrons is required. For this purpose, a radio frequency plasma source has also been developed [3, 4]. Dust plasma is characterized by charged grains immersed in plasma of electrons and ions. The grains could acquire charges of the order of 10^3 to 10^4 elementary charges and often become strongly coupled, which gives rise to novel phenomena such as the crystallization, phase transitions, and waves [5]. A variety of linear and nonlinear collective are known to occur in dust-contaminated plasma dusty plasma [6], and relative theoretical research has received new impulse, since roughly a decade ago, thanks to laboratory and space dusty plasma observations. An issue of particular importance in dusty plasma research is the formation of strongly coupled dusty plasma crystals by highly charged dust grains, typically in the sheath region above a horizontal negatively biased electrode in experiments [7]. A dusty plasma experiment with non-magnetic grains are presented for the dependence of the number density and lattice parameters of the dust layer on the ratio of the magnetic dipole-dipole force to electrostatic force between the grains and the orientation of the grain magnetic moment with respect to the layer [8]. Thermodynamic properties of a Yukawa

system consisting of dust particles in plasma are studied in presence of an external magnetic field. It is assumed that dust particles interact with each other by modified potential in presence of magnetic field. Accordingly, a modified expression for internal energy has been obtained [9]. Hypocycloid and epicycloids motions of irregular grain (pine pollen) are observed for the first time in unmagnetized dust plasma. Hypocycloid motions occur both inside and outside the glass ring which confines the grain [5].

Magnetite, Fe_3O_4 , with an inverse cubic spin structure ($a = 0,8396 \text{ nm}$) exhibits electrical conductivity ($\rho = 10 \text{ m}\Omega\cdot\text{cm}$ at $T = 300 \text{ K}$) due to a hopping of spin polarized electrons between ferrimagnetically ordered Fe_2^+ and Fe_3^+ ion states [10]. The nanoparticle powder of magnetite has already been synthesized for use as ferrofluid. Also due to their stability and nontoxic property Fe_3O_4 nanoparticles have been investigated for various medical applications. As an example, if magnetite nanoparticle is coated with proper organic compounds, the resulting material can be dispersed in water and is biocompatible. Due to the interaction of these magnetic nanoparticles with external field they may be guided by appropriate magnetic field to a specific point in body and used as contrast agent in magnetic resonance imaging or for targeted drug delivery. Such applications require the nanoparticles to be super paramagnetic. Moreover, the physical properties and, in particular, magnetic properties depend on the size of particles and their distribution [2].

Theory

The single Langmuir probe is a small conductor that can be introduced into the plasma to collect ion or electron current that flow into it in response to different voltage. The I-V graph is divided into

three regions ion saturation, transition, and electron saturation region [11] ,as shown in Fig. 1.

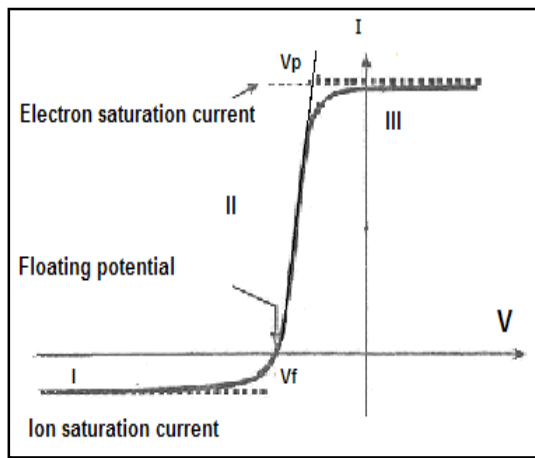


Fig.1: I-V characteristics of single Langmuir probe [12].

It is assumed that the probe current does not disturb the plasma. The probe diameter is less than the electron mean free path; the electrons are in thermal equilibrium among themselves at a temperature T_e with a Maxwellian kinetic energy distribution.

Region I: when V_p (probe potential) is made negative bias, electrons are repelled and only ions collected. The ion current passes through an area A in the plasma were determined from the ion currents in the ion saturation regions using the orbital motion limit (OML) probe theory. The advantage of using OML theory is that the ion density can be determined without the knowledge of the electron temperature. Here, it is assumed that the plasma is isotropic, the electron temperature is much higher than the ion temperature ($T_e \gg T_i$). The probe sheath is thick and non-collision assuming a Maxwellian energy distribution is in the unperturbed plasma. The following formula for a cylindrical probe is used to determine the ion current in the OML regime [11].

$$I_i = A_p n_i e \left(\frac{-eV_p}{8M_i} \right)^{1/2} \quad (1)$$

where I_i is the probe current (ion current), A_p is the surface area of the probe, M_i is the ionic mass (atomic mass unit, $1_{amu} = 1.67 \times 10^{-27} \text{kg}$ for proton), n_i is the ion density, V_p is probe potential (plasma potential).

In the short, typical I-Characteristics obtained with this arrangement as shown in Fig. 1. The I^2 vs. V_p , plot for the ion-collection range ($V_p < 0$) were obtained the slope of the linear region of these I^2 vs. V_p curves was used to calculate the ion density, without knowledge of the electron temperature according to the relation [11]:

$$n_i = 1.24 \times 10^{15} \frac{M_{amu}^{1/2} (slope)^{1/2}}{A_p} \quad (2)$$

The increasing of probe negative bias leads to repel all electrons and the current becomes pure ion current.

Region II : when the probe potential V_p is made less negative , probe collects both ions and electrons (the high thermal energy) as the potential (probe bias) is changed further in the positive direction, the ion and electron currents collected just cancel . This probe-plasma potential, V_f is the floating potential. For thermalized plasma, this voltage is approximately $1/2 kT$ (expressed in eV). Increasing probe potential beyond V_f results in a steep rise in electron current.

This current varied exponentially with probe bias voltage .this current eventually saturates at the plasma space potential value (V_p) due to space charge limitation in current collection.

In region, II the electron current is given [13].

$$I_e = \frac{A_p \cdot n_e \cdot e \cdot v_{th}}{4} \cdot \exp \frac{-eV}{kTe} \quad (3)$$

where v_{th} is the thermal velocity.

The electron temperature can therefore be calculated directly from the I-V characteristics of the probe. The slope yields the electron temperature [13]:

$$Slope = \frac{-e}{kTe} \quad (4)$$

Where T_e in (K).

$$\text{Slope} = \frac{1}{T_e} \quad (5)$$

Where T_e in (eV)

Methods of calculating the electron density described as following: in region III for positively biased of probe, the probe collects all the electrons and repels all the ions the electrons current collected is nearly constant. From this current, which is called the electron – saturation current I_s , the electron density can be calculated from the following relationship[14]:

$$I_s = \frac{n_e e A_p}{4} \left(\frac{2 k T_e}{m_e} \right)^{1/2} \quad (6)$$

The electron density is given by

$$n_e = 3.73 \times 10^{13} \frac{I_{sat}}{A_p^2 T_e^{1/2}} \quad (7)$$

where T_e is the electron temperature and the n_e is the electron number density. The floating potential can be calculated from the following equation, as the bias voltage at which $I_i + I_e = 0$, [15]

$$I_{is} = I_{es} \exp \left[\frac{e(V_f - V_p)}{k T_e} \right] \quad (8)$$

or

$$V_f = V_p + \left(\frac{k T_e}{e} \right) \ln \left[0.6 \left(\frac{2 \pi m_e}{m_i} \right)^{0.5} \right] \quad (9)$$

which are I_{es} and I_{is} called the electron-saturation current and the ion-saturation current respectively.

The characteristic shielding distance of the potential disturbance is the electron Debye length λ_{De} [16]:

$$\lambda_{De} = \left(\frac{\epsilon_0 k T_e}{e^2 n_e} \right)^{1/2} \quad (10)$$

Experiment set up

The vacuum chamber of this device is made of Pyrex cylindrical tube. This tube has two open ends closed by two stainless steel flange. One of it was connected to pumping systems, while the other was used to immerse the nitrogen gas, inside the chamber which consists of two disc aluminum electrodes (one of them used as cathode while the other used as the anode) 8 cm in diameter and 2 cm thickness. The inter distance between them is 8cm. Fig. 2 illustrates the experimental device with a discharge circuit.

Nitrogen plasmas are produced in the plasma chamber at plasma range from 0.1 torr to 1 torr. Iron (II and III) oxide is the chemical compound (Fe_3O_4) dust particles $\sim 185 \mu\text{m}$ in size are dropped from the top of chamber into plasma by a dust dropper (i.e. duster). This dust dropper consists of dust container having mesh and 3vdc motor. The electric motor works by remote control system. This motor gives two motions to the dust container which are rotation and vibration motions. The weight of the dust particles that immersed into the plasma is equal to 0.5 g. Fig. 3 shows the schematic diagram of vacuum chamber with electric circuit.

The glow discharge is formed between electrodes when a d.c. constant voltage of about 3 kV is applied between them. Therefore, the electrical breakdown is formed in nitrogen gas at relative pressures, of about ≈ 0.1 -1 torr.

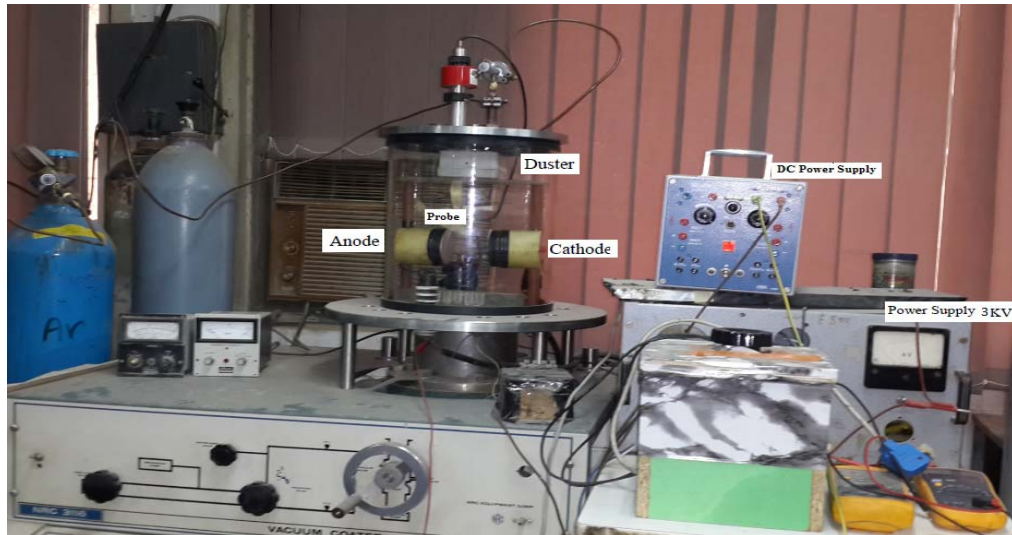


Fig.2: The photograph of the chamber system.

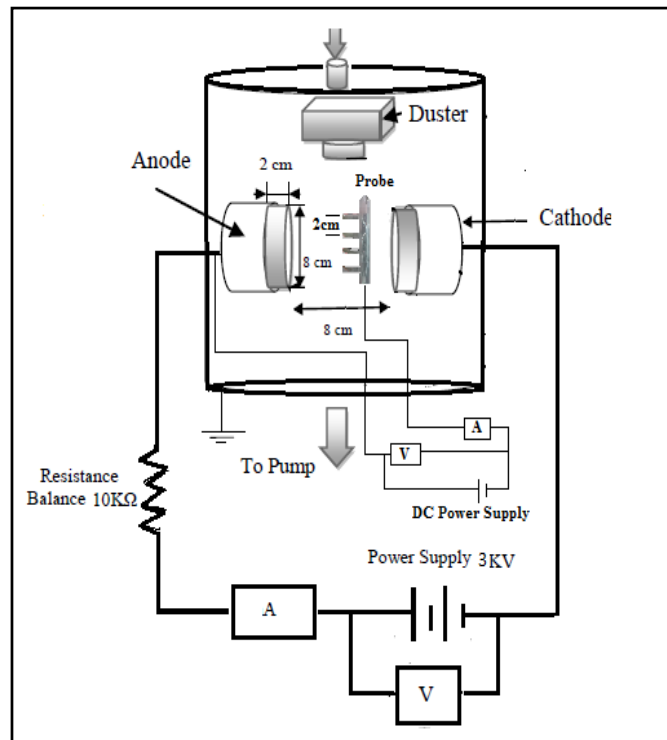


Fig.3: Schematic diagram of vacuum chamber with electric circuit.

Results and discussion

The d.c. glow discharge is produced when a d.c. constant potential of about 3kV is applied between two electrodes and the distance of 8 cm was from the cathode and anode. The plasma discharge is formed, the space charge is established and then the electrode potential will drop. Figs.4 and 5 show the current and voltage of discharge respectively. It is clear from these

figures, when the Fe_3O_4 dust is embedded, the discharge current decreases while the voltage of discharge was increasing. This behavior can be explained as; the increasing of losses of electrons causes by classical diffusion and collected of electrons on the dust surface causes to decrease the discharge current and increase of voltage discharge[17].

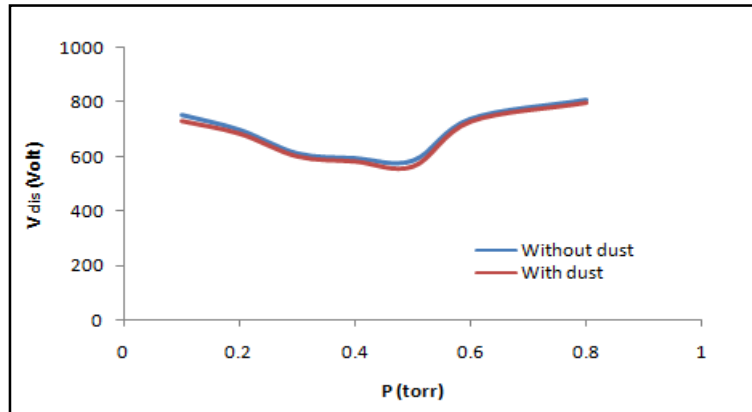


Fig.4: Schematic of the discharge voltage as a function of pressure at presence and absence of dust particles.

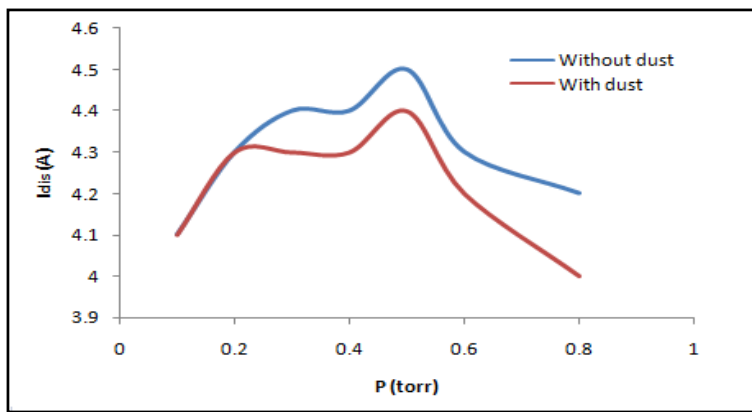


Fig.5: Schematic of the discharge current as a function of pressure at presence and absence of dust particles.

The plasma characteristic (such as V_p , V_f , I_{es} , n_i , n_e , T_e , λ_{De}) which werw found by using cylindrical Langmuir probes at pressure 0.5 torr at distance 4 cm from the cathode and anode (in half distance) were evaluated and investigated on the

plasma region. Fig. 6 shows the photographs for the four probes A, B, C, D at distance (1, 3, 5, 7) cm respectively from the edge of the diameter of the electrode.

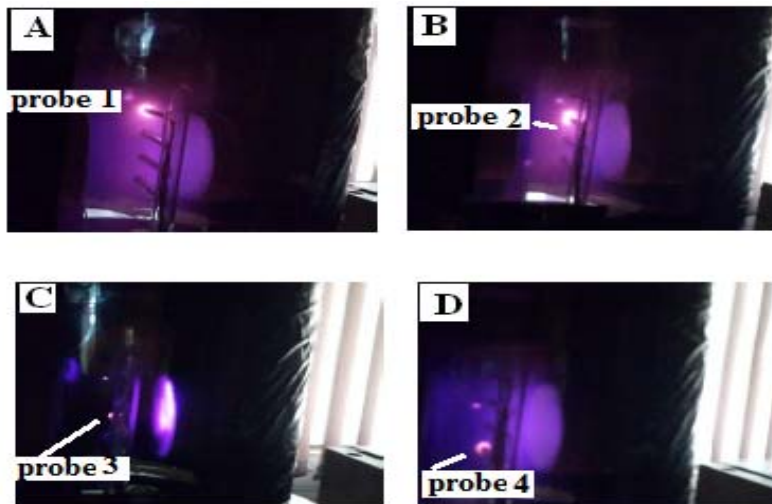


Fig.6: Photograph of the probeA, B, C and D at distance (1, 3, 5 and 7) cm with dust (Fe_3O_4).

The plasma potential with diameter position at different distance of the probe is illustrated in Fig. 7. The presence of Fe_3O_4 dust inside cathode sheath causes the plasma potential goes toward negative values. This behavior can be explained as, when the Fe_3O_4 dust embedded inside the plasma sheath, the electrons come first (because of their high mobility) after that the ions come later. Because of the polarity of charged dust depends on the emission of electrons, so that, the density of the ions decreases more than electrons density. Therefore, the potential of plasma becomes negative.

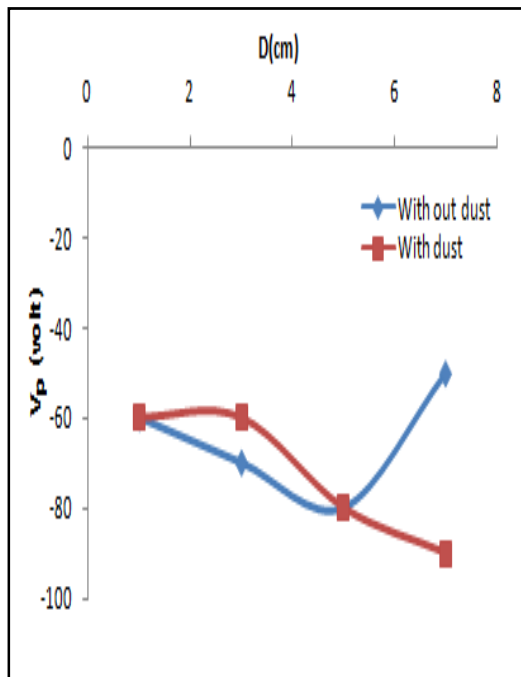


Fig.7: The plasma potential with Diameter position at different distances of the probe.

Moreover; Fig.8 illustrates the experimental data of electrons saturation current (I_{es}). As mention above, the presence of Fe_3O_4 dust in cathode sheath (cathode fall) collected the electrons according to that behavior, the saturation current of electron reduced.

Fig. 9 shows the floating potential (V_f) with different distances of the probe.

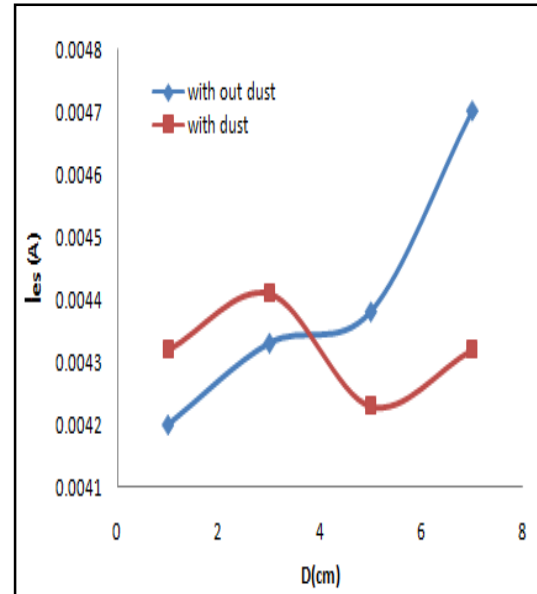


Fig.8: Diameter profile of electron saturation current at different distances of the probe.

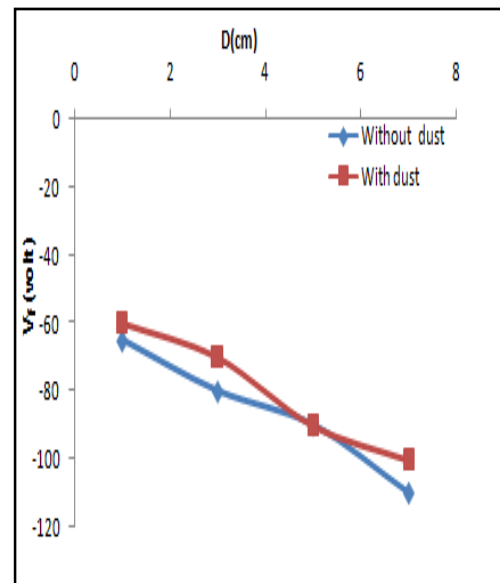


Fig.9: The floating potential with Diameter at different distances of the probe.

According to the Eq. (4) the electron temperature was measured from the slope of $\ln I_e - V$ curve of the probe characteristics. Fig.10 indicates the influence of Fe_3O_4 dust on radial profile of T_e . The figure shows that the pressure of dust particle reduces the electron temperature. This reduction may be

caused by; the electrostatic potential of dust grain surface causes to repel the electrons from it. Thus, the electron energy, furthermore, according to the experimental data of I_{es} from Fig. 8 and experimental data of T_e from Fig. 10, with Eq. (7) the radial distribution of n_e with and without dust particles are plotted in Fig. 11.

It can be explained from this figure, the losses of electrons caused by classical diffusion and the collision of electrons with other plasma particles (ions and neutral atoms) and the electrostatic potential of dust cause to reduce of electron density.

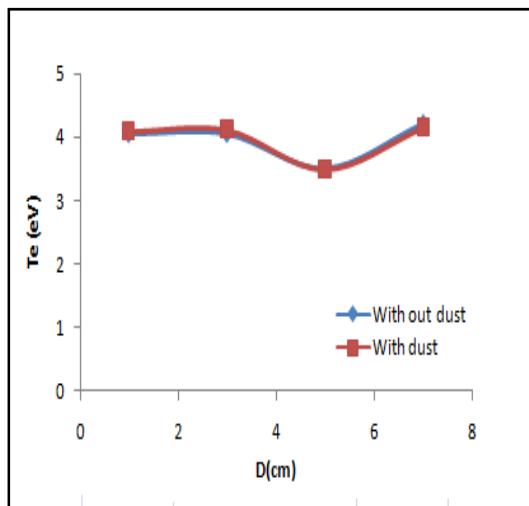


Fig.10: The electron temperature as a function of the Diameter position at different distances of the probe.

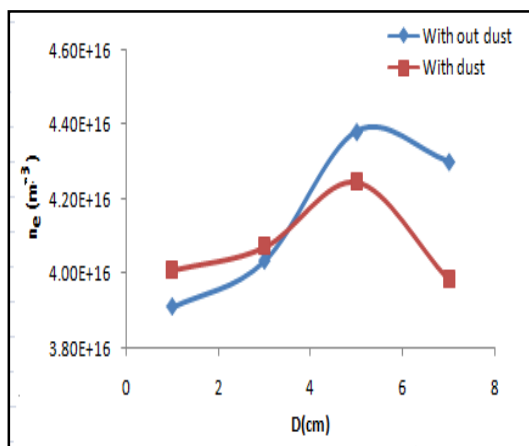


Fig.11: The electron density as a function of the Diameter position at different distances of the probe.

According to Eq. (2), the diameter profile of the ion density along the half distance 4 cm is shown in Fig.12. It is clear from this figure that, the ion density distribution is non-uniform with and without Fe_3O_4 dust along the plasma region in both distances. In addition, in the cathode sheath, the present of dust particles has influence on the ion density greater than in the plasma bulk [17].

Fig.13 shows the Debye length λ_{De} as a function of the diameter position at different distances of the probe. It is noticed from the figure that shape note that, a small decrease change in the Debye length in the case of Fe_3O_4 dust compared with the absence of dust.

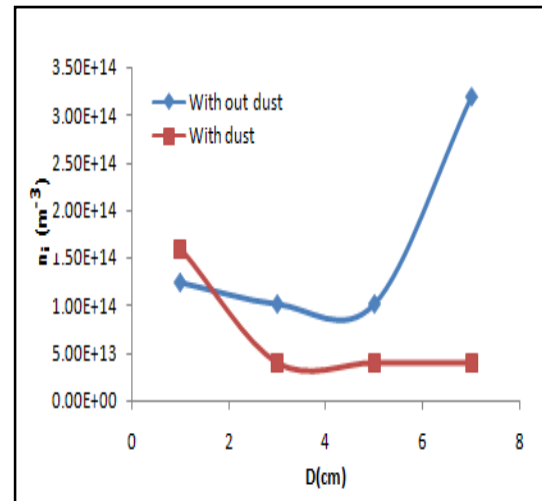


Fig.12: The ion density as a function of the Diameter position at different distances of the probe.

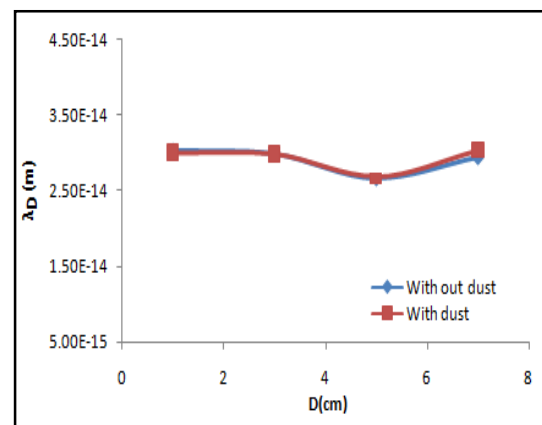


Fig.13: Debye length as a function of the Diameter position at different distances of the probes probe.

Conclusions

According to the above discussion, the following points can be concluded:

- The present of dust particle in the air plasma did not affect on Paschen minimum which is 0.5 torr without dust and with Fe₃O₄ dusty grains.
- The influence of dust particles on the plasma characteristics profile along the plasma region at pressure 0.5 torr was investigated. The current and voltage of discharges that present the experimentally observed decrease of discharge current and discharge voltage when the Fe₃O₄ dust was embedded.
- Plasma potential and the floating potential of probe become more negatively when the dust is immersed into plasma region. The electron density increases in the present of dust particle which leads to decrease the electron temperature and Debye length.

References

- [1] W. Oohara, D. Date, R. Hatakeyama, Phys. Rev. Lett. 95, 17 (2005) 175003.
- [2] K. Parvin, J. Ma, J. Ly X. C. Sun, D. E. Nikles K. Sun, L. M. Wang, Journal of Applied Physics 95, 11, June(2004)7121 -7123.
- [3] M.Stephen Rossnagel, J.Jerome Cuomo, D.William Westwood "Handbook of Plasma Processing Technology, Fundamentals" (Noyes Publications, Park Ridge, NJ, (1990).
- [4] T. Makabe, J. Matsui, K. Maeshige, Science and Technology of Advanced Materials, 2 (2001) 547-554.
- [5] J. H. Chu and I. Lin, Rev. Lett., 72 (1994) 4009-4012.
- [6] P. K. Shukla, A. A. Mamun," Introduction to Dusty Plasma Physics" (Institute of Physics, Bristol, (2002).
- [7] G. E. Mor, H. M. Thomas, M. Zuzic, in" Advances in Dusty Plasma Physics", Eds. P. K. Shukla, D. A. Mendis and T. Desai (World Scienti_c, Singapore, (1997).
- [8] M. Rosenberg, D. P. Sheehan, P. K. Shukla, IEEE, Trans. Plasma Sci., 34 (2006) 490-493.
- [9] M. Begum, S. Baruah, N. Das, Plasma Physics Reports, 40, 7 (2014) 583-590.
- [10] V. Lisauskas, B. Vengalis, K. Šliužienė, R. Butkutė, Physics and Chemistry of Solid State, 8, 3 (2007)638-640.
- [11] S.B.Singh, N. Chand, D.S.Patil, "Langmuir Probe Diagnostics of Microwave Electron Cyclotron Resonance (ECR)Plasma", Vacuum, 22, 1, 6 (2008) 372-377.
- [12] F. F. Chen, "Electric Probes, "Plasma Diagnostic Techniques", Ed. by Huddleston and Leonard (Academic Press, (1965).
- [13] Q. Adnan Abbas, Rabah A. Edan, Journal of Al-Nahrain University 17, 2 (2014)101-107.
- [14] L. Schott, "Plasma Diagnostics", edit by W. Lochte – Hot Greven (North Holland, Amsterdam, 668 (1968).
- [15] Q. Adnan Abbas, International Journal of Application or Innovation in Engineering and Management (IJAIEM), 2, 12, (2013) 470-478.
- [16] F.F.Chen, "Introduction to Plasma Physics and Controlled Fusion", Plenum Press, New York, (1984).
- [17] Q.Adnan Abbas, Eng. &Tech. Journal .31,Part (B), 5 (2013) 633-640.